ROYAL SOCIETY OPEN SCIENCE

rsos.royalsocietypublishing.org

Research

Cite this article: Wei X *et al*. 2017 From two-dimensional graphene oxide to three-dimensional honeycomb-like Ni_3S_2@graphene oxide composite: insight into structure and electrocatalytic properties. *R. Soc. open sci.* **4**: 171409.
http://dx.doi.org/10.1098/rsos.171409

Received: 26 September 2017
Accepted: 16 November 2017

Subject Category:
Chemistry

Subject Areas:
materials science

Keywords:
three-dimensional Ni_3S_2@ graphene oxide, catalysts, structure, electrocatalytic properties

Authors for correspondence:
Jie Yin
e-mail: yinjieily@163.com
Huawei Zhou
e-mail: zhouhuaweiopv@163.com

This article has been edited by the Royal Society of Chemistry, including the commissioning, peer review process and editorial aspects up to the point of acceptance.

Electronic supplementary material is available online at https://dx.doi.org/10.6084/m9.figshare.c.3944674.

ROYAL SOCIETY OF CHEMISTRY

THE ROYAL SOCIETY PUBLISHING

From two-dimensional graphene oxide to three-dimensional honeycomb-like Ni_3S_2@graphene oxide composite: insight into structure and electrocatalytic properties

Xinting Wei[1], Yueqiang Li[1,2], Wenli Xu[1], Kaixuan Zhang[1], Jie Yin[1], Shaozhen Shi[1], Jiazhen Wei[1], Fangfang Di[1], Junxue Guo[1], Can Wang[1], Chaofan Chu[1], Ning Sui[3], Baoli Chen[1], Yingtian Zhang[1], Hongguo Hao[1], Xianxi Zhang[1], Jinsheng Zhao[1], Huawei Zhou[1] and Shuhao Wang[1]

[1]School of Chemistry and Chemical Engineering; College of Materials Science and Engineering; Shandong Provincial Key Laboratory of Chemical Energy Storage and Novel Cell Technology, Liaocheng University, Liaocheng 252000, People's Republic of China
[2]Liaocheng Seismic Hydrochemistry Station, Liaocheng, People's Republic of China
[3]College of Materials Science and Engineering, Qingdao University of Science and Technology, Qingdao 266042, People's Republic of China

HZ, 0000-0002-9428-5400

Three-dimensional (3D) graphene composites have drawn increasing attention in energy storage/conversion applications due to their unique structures and properties. Herein, we synthesized 3D honeycomb-like Ni_3S_2@graphene oxide composite (3D honeycomb-like Ni_3S_2@GO) by a one-pot hydrothermal method. We found that positive charges of Ni^{2+} and negative charges of NO_3^- in $Ni(NO_3)_2$ induced a transformation of graphene oxide with smooth surface into graphene oxide with wrinkled surface (w-GO). The w-GO in the mixing solution of $Ni(NO_3)_2$/thioacetamide/H_2O

evolved into 3D honeycomb-like Ni_3S_2@GO in solvothermal process. The GO effectively inhibited the aggregation of Ni_3S_2 nanoparticles. Photoelectrochemical cells based on 3D Ni_3S_2@GO synthesized at 60 mM l^{-1} $Ni(NO_3)_2$ exhibited the best energy conversion efficiency. 3D Ni_3S_2@GO had smaller charge transfer resistance and larger exchange current density than pure Ni_3S_2 for iodine reduction reaction. The cyclic stability of 3D honeycomb-like Ni_3S_2@GO was good in the iodine electrolyte. Results are of great interest for fundamental research and practical applications of 3D GO and its composites in solar water-splitting, artificial photoelectrochemical cells, electrocatalysts and Li-S or Na-S batteries.

1. Introduction

Graphene is composed of SP^2 hybrid C atoms. The thickness of two-dimensional (2D) monolayer graphene is 3.35 Å. Six C atoms in the same plane bond with the adjacent C atoms in the sigma format, which makes the graphene have good structural rigidity. The orbit of surplus p is perpendicular to the graphene plane. The big π bonds are formed by overlapping of other p orbits. The electrons in big π bonds can move freely, which gives good conductivity to graphene. The unique monolayer graphene has a large theoretical specific surface area of about 2630 m^2 g^{-1}. It also has high conductivity, high electron mobility (15 000 cm^2 V^{-1} s^{-1}) [1], and thermal conductivity, quantum Holzer effect, quantum tunnelling effect [2], super mechanical properties [3], and so on. However, it lacks semiconductor properties, which limits its application in many fields.

Three-dimensional (3D) graphene composites have drawn increasing attention in energy storage/conversion applications due to their unique structures and properties [4–9]. Freestanding, lightweight 3D graphene networks as ultralight and flexible supercapacitor electrodes were prepared from pressed Ni foam [10]. A 3D graphene-based hierarchically porous carbon has been prepared by a dual template strategy and explored as an electrode for capacitive deionization [11]. A 3D carbon fibre/reduced graphene oxide composite textile was prepared by introducing 2D reduced graphene oxide interfaces into one-dimensional (1D) carbon fibre networks [12].

The composites of graphene and transition metal complexes (TMC) possess electrical conductivity, thermal conductivity, structure stability and excellent catalytic activity. The structures of TMC/graphene composite material have four categories: 0D/2D (zero-dimensional TMC/two-dimensional graphene), 1D/2D (one-dimensional TMC/two-dimensional graphene), 2D/2D (two-dimensional TMC/two-dimensional graphene) and 3D (TMC/three-dimensional graphene).

3D NiS/G composite and 3D CoS/G composite were prepared by three steps: growing graphene by chemical vapour deposition, coating precursors and further annealing [13]. The dye-sensitized solar cells (DSCs) with 3D NiS/G composite and 3D CoS/G composite counter electrodes showed good electrocatalytic activity and photovoltaic conversion efficiencies of 5.04% and 5.25%, respectively. We previously reported that unique ZnS nanobuns decorated with 2D reduced graphene oxide were synthesized using one-pot solvothermal method. Graphene in ZnS@GO remained in 2D structures (flake-like shape with few wrinkles). Herein, we synthesized 3D honeycomb-like Ni_3S_2@graphene oxide composite (3D honeycomb-like Ni_3S_2@GO) by a one-pot hydrothermal method. We study the structural characteristics of 3D honeycomb-like Ni_3S_2@GO evolved from 2D graphene oxide. The electrocatalytic characteristics of 3D honeycomb-like Ni_3S_2@GO for iodine reduction reaction are investigated by electrochemical impedance (EIS) and Tafel polarization. The effects of 3D honeycomb-like Ni_3S_2@GO structure on photovoltaic parameters are also investigated.

2. Material and methods

2.1. Preparation of pure Ni_3S_2 block

Typically, 0.0017 mol $Ni(NO_3)_2{\cdot}6H_2O$ was dissolved in 30 ml deionized water by vigorous agitation. Thioacetamide (TAA) (0.023 mol) was dissolved in 30 ml deionized water by vigorous agitation. The above two solutions were mixed. The mixture was stirred for 0.5 h at room temperature and then transferred into a Teflon-lined autoclave. After being heated at 200°C for 24 h, the product was cooled to room temperature naturally. The product was washed three times with water and ethanol.

2.2. Preparation of three-dimensional honeycomb-like Ni_3S_2@graphene oxide

Specific synthesis method of GO could be seen in our previous literature [14–16]. GO (1.125 g 1 wt%) was dispersed in 10 ml deionized water by ultrasound. 0.0017 mol $Ni(NO_3)_2{\cdot}6H_2O$ was dissolved in 30 ml deionized water by vigorous agitation. TAA (0.023 mol) was dissolved in 20 ml deionized water by vigorous agitation. The above three solutions were mixed. The mixture was stirred for 0.5 h at room temperature and then transferred into a Teflon-lined autoclave. After being heated at 200°C for 24 h, the product was cooled to room temperature naturally. The product was washed three times with water and ethanol.

2.3. Photoanode preparation and cell fabrication

A 12 µm thick layer was deposited on fluorine-doped tin oxide glass by printing 20 nm-sized TiO_2 particles (P25, Degussa, Germany) [15,17]. The obtained film was sintered at 500°C. After cooling to 90°C, the TiO_2 films were immersed in a solution of N719 dye (5×10^{-4} M) in acetonitrile/*tert*-butyl alcohol (1 : 1 volume ratio) for 20 h. The triiodide/iodide electrolyte for cell testing includes LiI (0.03 M), 1-butyl-3-methylimidazolium iodide (0.6 M), I_2 (0.03 M), 4-*tert*-butylpyridine (0.5 M), guanidinium thiocyanate in acetonitrile (0.1 M). DSCs were assembled by a TiO_2 photoanode with the corresponding counter electrode sandwiching the redox couple in the electrolyte. Symmetrical cells with an effective area of 0.64 cm^2 were analysed by a Tafel-polarization test and by EIS experiments.

2.4. Characterization

To analyse as-synthesized composite electrocatalyst, X-ray diffraction (XRD) patterns were acquired using a PANalytical X'Pert diffractometer (Cu Kα radiation at $\lambda = 1.5406$ Å) sampling at 5° min^{-1}, 36 kV and 20 mA. As-prepared micro- or nanostructures were characterized and analysed by scanning electron microscopy (SEM; Nova Nano SEM 450). The photocurrent–voltage performance of DSCs with 0.16 cm^2 photoanode film was measured without metal mask by a Keithley digital source meter (Keithley 2400, USA) equipped with a solar simulator (IV5, PV Measurements, Inc., USA). EIS and Tafel experiments were done with symmetrical electrodes in the dark using an electrochemical workstation (CHI760 Chenhua, China). Cyclic voltammetry (CV) was performed in a three-electrode configuration. The triiodide/iodide electrolyte for CV testing includes LiI (2 mM), $LiClO_4$ (20 mM) and I_2 (0.2 mM).

3. Results and discussion

The graphene oxide prepared by the Hummers method usually contains a large number of functional groups. The functional groups (hydroxyl and carboxyl groups) on the graphene surface can make graphene more compact and stable when graphene is combined with other materials. As shown in figure 1, graphene oxide prepared by us can be well dispersed in H_2O to form a homogeneous dispersion. The graphene oxide in H_2O (GO/H_2O) can be stable for several months or longer without delamination. The reason for this is the strong hydrogen bonding between hydroxyl and carboxyl groups on the surface of graphene oxide and H_2O. Therefore, the surface of the graphene oxide in H_2O is relatively smooth, rather than wrinkled. The graphene oxide with a smooth surface is s-GO. When TAA was added into GO/H_2O, no obvious change was observed in the homogeneous dispersion. However, when $Ni(NO_3)_2$ solution or mixed solution of $Ni(NO_3)_2$ and TAA were added into GO/H_2O, homogeneous dispersion shows lots of flocculent graphene oxide immediately, as shown in figure 1. Because lots of positive charges of Ni^{2+} and negative charges of NO_3^- in $Ni(NO_3)_2$ destroy the hydrogen bonding between graphene oxide and H_2O, the surface of flocculent graphene oxide should be wrinkled rather than smooth, as shown in figure 1. The graphene oxides with wrinkled surface were named w-GO. SEM of w-GO is shown in electronic supplementary material, figure S1. w-GO has two advantages: on the one hand, it can keep the 2D structure of graphene; on the other hand, the wrinkles on the surface can increase the physical and chemical properties in graphene devices. The w-GO suspension is transferred into a Teflon-lined autoclave. After crystallizing and cross-linking of w-GO suspension at 200°C for 24 h, 3D honeycomb-like structures of Ni_3S_2@GO were formed, as shown in figure 1.

We investigated the effect of different concentrations of $Ni(NO_3)_2$ on the morphology of Ni_3S_2@GO. As can be seen from figure 2, the microstructures of all the synthesized Ni_3S_2@GO samples obtained using 6, 30 and 60 mM l^{-1} $Ni(NO_3)_2$ have 3D honeycomb-like structures. This kind of 3D honeycomb-like structure possessed larger specific surface area and more surface catalytic activity sites. In addition,

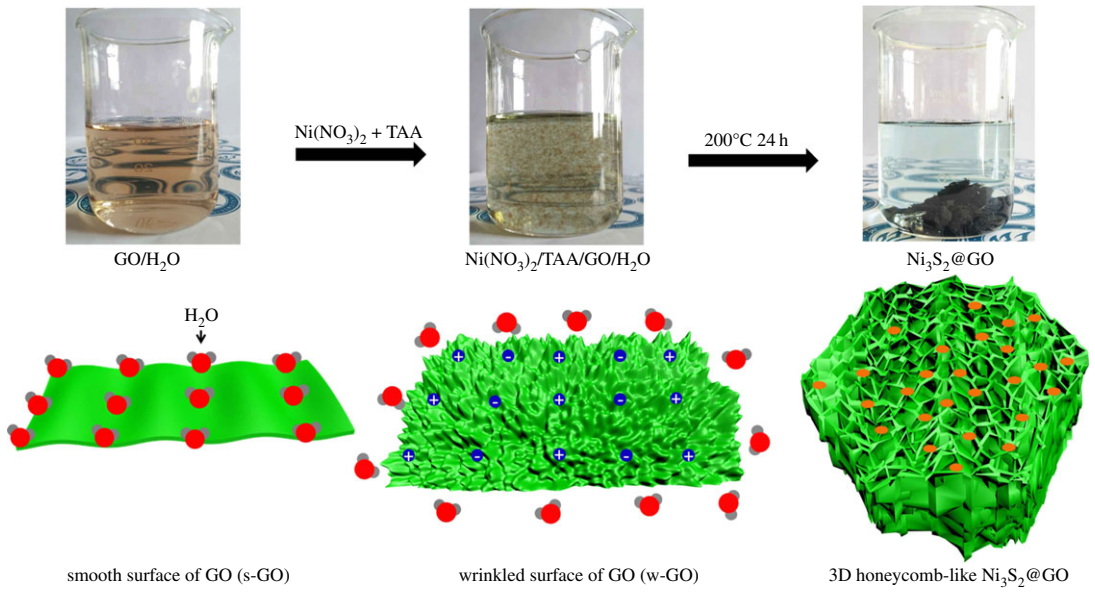

Figure 1. Picture and structural evolution of 3D honeycomb-like Ni_3S_2@GO from graphene oxide with smooth surface and graphene oxide with wrinkled surface.

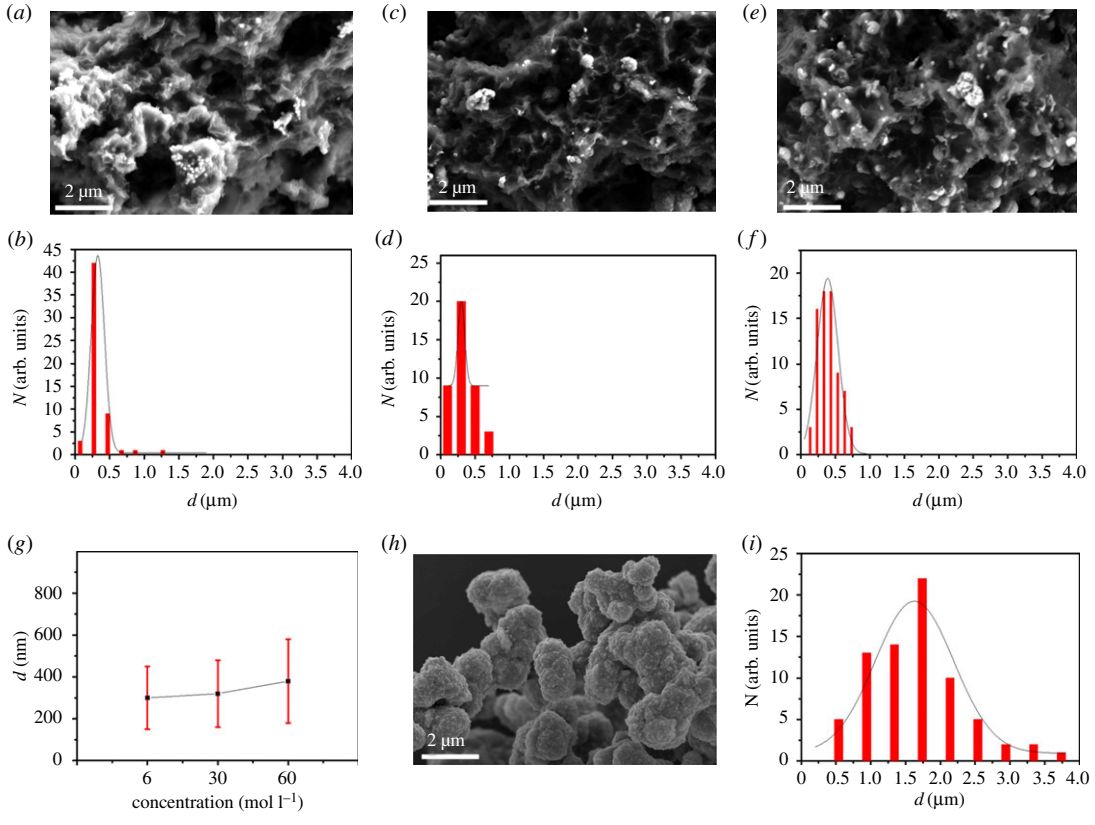

Figure 2. (*a*,*b*) SEM image and size distribution for 3D honeycomb-like Ni_3S_2@GO synthesized under 6 mM l^{-1} $Ni(NO_3)_2$; (*c*,*d*) SEM image and size distribution for 3D honeycomb-like Ni_3S_2@GO synthesized under 30 mM l^{-1} $Ni(NO_3)_2$; (*e*,*f*) SEM image and size distribution for 3D honeycomb-like Ni_3S_2@GO synthesized under 60 mM l^{-1} $Ni(NO_3)_2$; (*g*) the relationship between the size of Ni_3S_2 on graphene surface and the concentration of $Ni(NO_3)_2$; (*h*,*i*) SEM image and size distribution for pure Ni_3S_2 synthesized under 30 mM l^{-1} $Ni(NO_3)_2$.

the coupling between the walls of w-GO and Ni_3S_2 will play the role of synergistic catalysis. There are few Ni_3S_2 nanoparticles on the 3D honeycomb-like Ni_3S_2@GO under 6 mM l^{-1} $Ni(NO_3)_2$. The size of Ni_3S_2 nanoparticles on the 3D honeycomb-like Ni_3S_2@GO is approximately 300 nm (figure 2*a*,*b*). When the concentration of $Ni(NO_3)_2$ is 30 mM l^{-1}, the numbers of Ni_3S_2 nanoparticles on the 3D

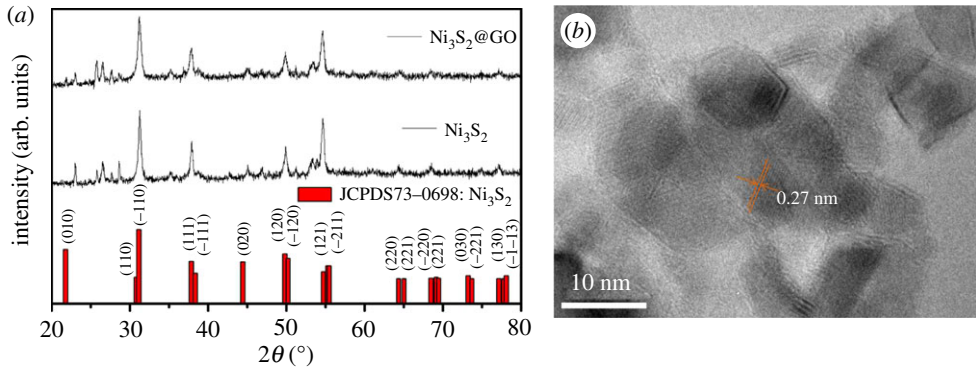

Figure 3. (*a*) XRD patterns of as-prepared 3D honeycomb-like Ni_3S_2@GO and pure Ni_3S_2 synthesized under 30 mM l^{-1} $Ni(NO_3)_2$; (*b*) high-resolution transmission electron micrograph of as-prepared 3D honeycomb-like Ni_3S_2@GO under 30 mM l^{-1} $Ni(NO_3)_2$.

honeycomb-like Ni_3S_2@GO are increased. The size of Ni_3S_2 nanoparticles on the 3D honeycomb-like Ni_3S_2@GO is approximately 320 nm, as shown in figure 2*c*,*d*. The numbers of the Ni_3S_2 nanoparticles on the 3D honeycomb-like Ni_3S_2@GO under 60 mM l^{-1} are more than those under 6 and 30 mM l^{-1} $Ni(NO_3)_2$. The size of Ni_3S_2 nanoparticles on the 3D honeycomb-like Ni_3S_2@GO is approximately 380 nm (figure 2*e*,*f*). As shown in figure 2*g*, the size of graphene surface Ni_3S_2 is gradually increased with increasing concentration of $Ni(NO_3)_2$. The SEM results of pure Ni_3S_2 material synthesized under 30 mM l^{-1} $Ni(NO_3)_2$ are shown in figure 2*h*. It can be seen that the pure Ni_3S_2 block was larger than Ni_3S_2 in Ni_3S_2@GO. The size of Ni_3S_2 block is approximately 1.7 µm, as shown in figure 2*i*. The results suggested that the presence of graphene significantly inhibits aggregation of Ni_3S_2 nanoparticles, which is consistent with our previous findings [11].

The XRD pattern of the 3D honeycomb-like Ni_3S_2@GO powder is shown in figure 3*a*. In order to classify the diffraction peaks, we synthesized pure Ni_3S_2 as the contrast. The diffraction pattern of 3D honeycomb-like Ni_3S_2@GO is consistent with that of pure Ni_3S_2. All of the peaks are in accordance with the Ni_3S_2 standard card (PDF#73-0698). The strong diffraction peaks at 31.26° and 54.7° corresponded to (−110) and (−211) crystal planes. The other diffraction peaks at 23.04°, 37.94° and 49.88° corresponded to (010), (111), (120) crystal planes. From further structural analysis by high-resolution transmission electron microscopy, the lattice spacing of Ni_3S_2 on Ni_3S_2@GO is 0.27 nm, which is close to [−110] spacing of Ni_3S_2 (PDF#73-0698).

3D honeycomb-like Ni_3S_2@GO synthesized by different concentrations of $Ni(NO_3)_2$ was prepared in thin film by the spraying method and used as a counter electrode in DSCs. Meanwhile, pyrolytic platinum was prepared to be used as a reference. The normalized power conversion efficiency is shown in figure 4*a*. The results indicated that the highest energy conversion efficiency is based on 3D honeycomb-like Ni_3S_2@GO synthesized by 30 mM l^{-1} $Ni(NO_3)_2$. The effect of 3D honeycomb-like Ni_3S_2@GO structure synthesized by different $Ni(NO_3)_2$ concentration on open circuit voltage (V_{oc}), short circuit current density (J_{sc}) and fill factor is shown in electronic supplementary material, figures S2, S3 and S4. The best energy conversion efficiency based on 3D Ni_3S_2@GO synthesized at 60 mM l^{-1} $Ni(NO_3)_2$ is shown in electronic supplementary material, figure S5. To investigate the reason for the good performance of 3D honeycomb-like Ni_3S_2@GO materials in DSCs, EIS and Tafel polarization were carried out. EIS is an electrochemical method widely used for the characterization of counter electrode. Figure 4*b* is a typical Nyquist diagram. Each Nyquist diagram usually consists of two semicircles. The resistance of left semicircle starting on *X*-axis represented the series resistance (R_s). The value of left semicircle diameter represented charge transfer resistance (R_{ct}) between the electrode and electrolyte. R_{ct} occurs in the high-frequency region and is closely related to the electrocatalytic properties. According to the symmetrical cell equivalent circuit diagram in figure 4*b*, the EIS parameters obtained by Z-View software are listed in table 1.

The values of R_s for 3D honeycomb-like Ni_3S_2@GO and pure Ni_3S_2 in I^-/I_3^- electrolyte system are 38.19 Ω and 50.72 Ω, respectively. The main reason for the smaller R_s of 3D honeycomb-like Ni_3S_2@GO is the high conductivity of graphene in composites. The value of R_{ct} for 3D honeycomb-like Ni_3S_2@GO is 40.29 Ω, which is much smaller than that of pure Ni_3S_2 (106.4 Ω). The results indicated that 3D honeycomb-like Ni_3S_2@GO exhibited better electrocatalytic activity than pure Ni_3S_2 for the reduction reaction of iodine. The frequency at highest point of left semicircle for Ni_3S_2 is

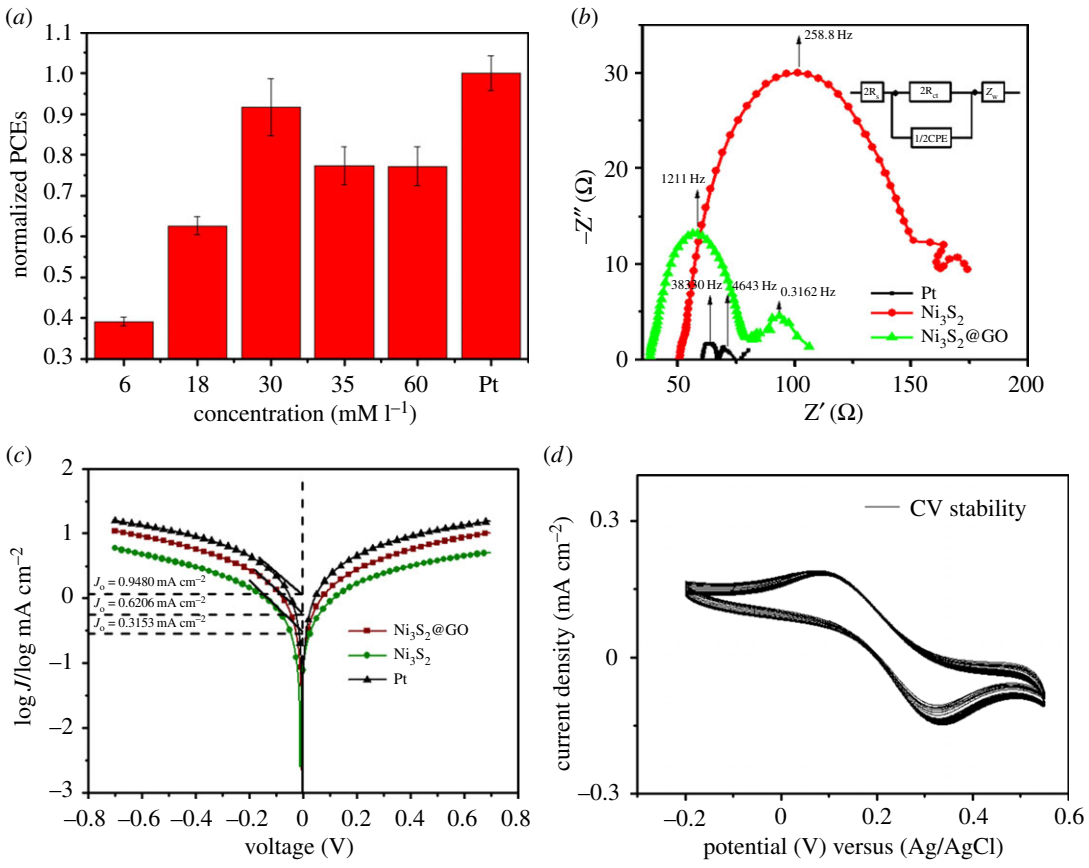

Figure 4. (*a*) The normalized power conversion efficiency (PCE) based on 3D honeycomb-like Ni_3S_2@GO synthesized by different concentration of $Ni(NO_3)_2$; (*b*) EIS of symmetrical cells fabricated with two identical 3D honeycomb-like Ni_3S_2@GO or pure Ni_3S_2 (synthesized by 30 mM l^{-1} $Ni(NO_3)_2$) under the bias voltage with open voltage corresponding to photovoltaic devices; (*c*) Tafel polarization curves of symmetrical cells fabricated with two identical 3D honeycomb-like Ni_3S_2@GO or pure Ni_3S_2 (synthesized by 30 mM l^{-1} $Ni(NO_3)_2$) under the bias voltage with open voltage corresponding to photovoltaic devices; (*d*) the cyclic stability of 3D honeycomb-like Ni_3S_2@GO (synthesized by 30 mM l^{-1} $Ni(NO_3)_2$) in the iodine electrolyte.

Table 1. Series resistance (R_s), charge transfer resistance (R_{ct}) and exchange current density based on the symmetrical cells of 3D honeycomb-like Ni_3S_2@GO, Ni_3S_2 (synthesized by 30 mM l^{-1} $Ni(NO_3)_2$) and Pt in the iodine electrolyte.

electrolytes	CEs	R_s/Ω	R_{ct}/Ω	J_0/mA cm^2
I^-/I_3^-	Ni_3S_2@GO	38.19	40.29	0.6206
	Ni_3S_2	50.72	106.4	0.3153
	Pt	60.86	6.866	0.9480

258.8 Hz, which corresponds to a time constant of 0.003864 s. The frequency at highest point of left semicircle for 3D honeycomb-like Ni_3S_2@GO is 1211 Hz, which corresponds to a time constant of 0.0008921 s. The time constants also indicated that the catalytic performance of 3D honeycomb-like Ni_3S_2@GO was better than that of pure Ni_3S_2. R_{ct} and the exchange current density (J_0) in Tafel was inversely proportional, according to $R_{ct} = RT/nFJ_0$. The values of J_0 for 3D honeycomb-like Ni_3S_2@GO and pure Ni_3S_2 are 0.6317 mA cm^{-2} and 0.36625 mA cm^{-2}, respectively. The result indicated that the iodine reduction reaction has faster electron exchange on the surface of 3D honeycomb-like Ni_3S_2@GO, which is consistent with the EIS results. The cyclic stability of 3D honeycomb-like Ni_3S_2@GO in the iodine electrolyte is shown in figure 4*d*. The current density and the potential position had no significant change, which indicated the good stability of 3D honeycomb-like Ni_3S_2@GO in the iodine electrolyte.

4. Conclusion

In sum, 3D honeycomb-like Ni_3S_2@GO was synthesized by a one-pot hydrothermal method. The positive charges of Ni^{2+} and negative charges of NO_3^- in $Ni(NO_3)_2$ induced a transformation of s-GO into w-GO. The GO can effectively inhibit the aggregation of Ni_3S_2 nanoparticles. 3D honeycomb-like Ni_3S_2@GO exhibited good electrocatalytic activity and photoelectrochemical performance. These findings are of great interest for fundamental research and practical applications of 3D graphene oxides and their composites.

Data accessibility. Additional data are in the electronic supplementary material.

Authors' contributions. J.Y. and H.Z. designed the study, interpreted the results and wrote the manuscript. X.W., Y.L., W.X., K.Z., S.S., J.W., F.D., J.G., C.W. and C.C. prepared all samples for analysis. N.S., B.C., Y.Z., H.H., X.Z., J.Z. and S.W. collected and analysed the data. All authors gave their final approval for publication.

Competing interests. We declare we have no competing interests.

Funding. This work was financially supported by Shandong Province Natural Science Foundation (grant nos. ZR2016BQ20; BS2015NJ013; ZR2014BQ010; ZR2016BQ21), colleges and universities in Shandong Province science and technology projects (grant no. J16LC05), Science and Technology Innovation Foundation for the University or College Students (grant no. 26312160502), National Science and Technology Innovation Foundation for the University or College Students (grant no. 201510447021), Research Fund for the Doctoral Program of Liaocheng University (grant no. 31805), National Natural Science Foundation of China (grant nos. 21503104; 21601078; 21401095), National Basic Research Program of China (grant no. 2011CBA00701).

References

1. Cheianov VV, Fal'ko VI. 2006 Selective transmission of dirac electrons and ballistic magnetoresistance of n-p junctions in graphene. *Phys. Rev. B* **74**, 041403. (doi:10.1103/PhysRevB.74.041403)
2. Katsnelson MI. 2007 Graphene: carbon in two dimensions. *Mater. Today* **10**, 20–27. (doi:10.1016/S1369-7021(06)71788-6)
3. Lee C, Wei XD, Kysar JW, Hone J. 2008 Measurement of the elastic properties and intrinsic strength of monolayer graphene. *Science* **321**, 385–388. (doi:10.1126/science.1157996)
4. Luo B, Zhi LJ. 2015 Design and construction of three dimensional graphene- based composites for lithium ion battery applications. *Energy Environ. Sci.* **8**, 456–477. (doi:10.1039/C4EE02578D)
5. Mao S, Lu GH, Chen JH. 2015 Three-dimensional graphene-based composites for energy applications. *Nanoscale* **7**, 6924–6943. (doi:10.1039/C4NR06609J)
6. Shehzad K, Xu Y, Gao C, Duan XF. 2016 Three-dimensional macro-structures of two-dimensional nanomaterials. *Chem. Soc. Rev.* **45**, 5541–5588. (doi:10.1039/C6CS00218H)
7. Shehzad K *et al.* 2017 Designing an efficient multimode environmental sensor based on graphene-silicon heterojunction. *Adv. Mater. Technol.* **2**, 1600262. (doi:10.1002/admt.201600262)
8. Xu Y *et al.* 2017 Solvent-based soft-patterning of graphene lateral heterostructures for broadband high-speed metal-semiconductor-metal photodetectors. *Adv. Mater. Technol.* **2**, 1600241. (doi:10.1002/admt.201600241)
9. Ren Z, Meng N, Shehzad K, Xu Y, Qu S, Yu B, Luo JK. 2015 Mechanical properties of nickel-graphene composites synthesized by electrochemical deposition. *Nanotechnology* **26**, 065706. (doi:10.1088/0957-4484/26/6/065706)
10. He Y, Chen W, Li X, Zhang Z, Fu J, Zhao C, Xie E. 2013 Freestanding three-dimensional graphene/MnO_2 composite networks as ultra light and flexible supercapacitor electrodes. *ACS Nano* **7**, 174–182. (doi:10.1021/nn304833s)
11. Wen XR, Zhang DS, Yan TT, Zhang JP, Shi LY. 2013 Three-dimensional graphene-based hierarchically porous carbon composites prepared by a dual-template strategy for capacitive deionization. *J. Mater. Chem. A* **1**, 12 334–12 344. (doi:10.1039/C3TA12683H)
12. Li J, Bi S, Mei B, Shi F, Cheng W, Su X, Hou G, Wang J. 2017 Effects of three-dimensional reduced graphene oxide coupled with nickel nanoparticles on the microwave absorption of carbon fiberbased composites. *J. Alloys Compd.* **717**, 205–213. (doi:10.1016/j.jallcom.2017.03.098)
13. Bi H, Zhao W, Sun S, Cui H, Lin T, Huang F, Xie X, Jiang M. 2013 Graphene films decorated with metal sulfide nanoparticles for use as counter electrodes of dye-sensitized solar cells. *Carbon* **61**, 116–123. (doi:10.1016/j.carbon.2013.04.075)
14. Yin J, Wang J, Li HY, Ma HY, Li WZ, Shao X. 2014 Unique ZnS nanobuns decorated with reduced graphene oxide as an efficient and low-cost counter electrode for dye-sensitized solar cells. *J. Energy Chem.* **23**, 559–563. (doi:10.1016/S2095-4956(14)60185-6)
15. Zhou H *et al.* 2016 Earth-abundant and nano-micro composite catalysts of Fe_3O_4@reduced graphene oxide for green and economical mesoscopic photovoltaic devices with high efficiencies up to 9%. *J. Mater. Chem. A* **4**, 67–73. (doi:10.1039/C5TA06525A)
16. Yin J, Zhou H, Liu Z, Nie Z, Li Y, Qi X, Chen B, Zhang Y, Zhang X. 2016 Indium- and platinum-free counter electrode for green mesoscopic photovoltaics through graphene electrode and graphene composite catalysts: interfacial compatibility. *ACS Appl. Mater. Interfaces* **8**, 5314–5319. (doi:10.1021/acsami.5b11850)
17. Shi Y, Zhu C, Wang L, Zhao C, Li W, Fung KK, Ma T, Hagfeldt A, Wang N. 2013 Ultrarapid sonochemical synthesis of ZnO hierarchical structures: from fundamental research to high efficiencies up to 6.42% for quasi-solid dye-sensitized solar cells. *Chem. Mater.* **25**, 1000–1012. (doi:10.1021/cm400220q)